applied sciences

IMPACT FACTOR 2.5

CITESCORE 5.3

Article

The Optimization of Frequency Distribution Based on Genetic Algorithm for Space Gravitational Wave Observatories

Lixiao Zeng, Haojie Li, Weilai Yao, Jianyu Wang and Xindong Liang

MDPI

https://doi.org/10.3390/app14124963

applied sciences

MDPI

Article

The Optimization of Frequency Distribution Based on Genetic Algorithm for Space Gravitational Wave Observatories

Lixiao Zeng [1,2,3], Haojie Li [1,2,3,4], Weilai Yao [1,2,3,4], Jianyu Wang [1,2,3,4,5] and Xindong Liang [1,2,3,5,*]

1 Taiji Laboratory for Gravitational Wave Universe, School of Physics and Optoelectronic Engineering, Hangzhou Institute for Advanced Study, Hangzhou 310012, China; zenglixiaostu@163.com (L.Z.)
2 University of Chinese Academy of Sciences, Beijing 100049, China
3 Key Laboratory of Gravitational Wave Precision Measurement of Zhejiang Province, Hangzhou Institute for Advanced Study, Hangzhou 310012, China
4 Key Laboratory of Space Active Opto-Electronic Technology and Systems, Shanghai Institute of Technical Physics, Chinese Academy of Sciences, Shanghai 200083, China
5 Research Center for Intelligent Sensing, Zhejiang Laboratory, Hangzhou 311100, China
* Correspondence: liangxindong@ucas.ac.cn

Abstract: The three spacecraft of the space gravitational wave antenna employ heterodyne interferometry to mitigate the effects of Doppler shift. Constrained by laser relative intensity noise (RIN) and the sampling frequency constraints of phase readout circuits, the widespread adoption of fixed offset frequencies effectively regulates the frequency of heterodyne interferometric beat notes within a reasonable frequency domain of [5 MHz, 25 MHz]. In this work, a high-precision fitness genetic algorithm for heterodyne interferometry is utilized to generate the initial offset frequency distribution scheme. To address issues with unreasonable switching times and offset frequency settings in the initial scheme for partial frequency domains, optimization strategies are proposed from three aspects: frequency domain selection extension, switch times control, and numerical low frequency. Results demonstrate that the optimization of frequency domain selection extension narrows the reasonable frequency domain to [5 MHz, 15 MHz] and [7 MHz, 17 MHz]. Optimization of switch times control ensures that switching times of offset frequency distribution scheme generated under the settings of [6 MHz, 17 MHz] and wider frequency domains can be controlled within a reasonable range of 6 to 13 times. Fixed offset frequency settings are generally reduced by 24.3% after low-frequency optimization. This methodology and result can provide a reliable reference for Program Taiji and even related space gravitational wave antenna projects.

Keywords: gravitational wave antenna; Taiji project; laser heterodyne interferometry; algorithm optimization

Citation: Zeng, L.; Li, H.; Yao, W.; Wang, J.; Liang, X. The Optimization of Frequency Distribution Based on Genetic Algorithm for Space Gravitational Wave Observatories. *Appl. Sci.* **2024**, *14*, 4963. https://doi.org/10.3390/app14124963

Academic Editor: John Xiupu Zhang

Received: 20 April 2024
Revised: 30 May 2024
Accepted: 3 June 2024
Published: 7 June 2024

1. Introduction

The space gravitational wave [1,2] antenna program Taiji consists of three spacecrafts flying in a heliocentric [3], with separations of $L = 3 \times 10^9$ m [4]. Each spacecraft (SC) contains two proof masses that are shielded from external disturbances. Bidirectional laser links are maintained between all SC in the constellation for exchanging laser beams to interferometrically measure the pathlength variations at the picometer level caused by gravitational waves [5,6]. During the mission operation, spaceborne interferometers will be affected by Doppler shifts [7]. Thus, the interferometers in Taiji are based on heterodyne interferometry, where two laser beams from local and remote SC are combined to yield a beat note, the phase of which is used to lock and track the remote laser [8]. However, the Doppler shift due to the inter-spacecraft motion varies with time. This will cause the beat frequency to enter some disallowed frequency bands over the five-year operational cycle and stop probing [9]. In particular, the laser relative intensity noise (RIN) [10] and phase readout circuit sampling frequency [11,12] limit the minimum and maximum of the

allowed frequency bands respectively. For the Taiji program, The lower bound of the beat frequency is 5 MHz, and the upper is 25 MHz [13]. In order to address this issue, current research commonly adds offset frequencies into the interferometric link to control the beat frequency [14,15].

The fixed offset frequency method is mainly used to control the beat frequency within the reasonable range of [5 MHz, 25 MHz]. A crucial challenge of the method is the reasonable distribution of the offset frequency. Once the current offset frequency is unable to keep the beat frequency within a reasonable range, the offset frequency needs to be switched, and the interferometry needs to be restarted, which will inevitably lead to the interruption of observation data. Barke [9] proposed a frequency distribution scheme of [7 MHz, 23 MHz], requiring 24 switches. The offset frequencies theoretically did not require changing for a maximum of 177 days within the specified constraints. Due to the need for prolonged uninterrupted detection by the system, excessive switching and insufficient duration can lead to probing errors. Additionally, Zhang utilized a linear programming (LP) algorithm [13] and a two-stage optimization algorithm [14] to solve the setting strategy of the offset frequencies. The LP algorithm provided an offset frequency distribution scheme that can remain unchanged for up to 1931 days over a six-year period. The two-stage optimization algorithm reduced the upper bound to 16 MHz and provided a scheme that the offset frequency changes nine times with a minimum and maximum offset frequency duration of 90 days and 713 days, respectively. Based on the above research, this paper makes appropriate improvements. A high-precision fitness genetic algorithm is adopted to generate an initial distribution scheme. Three optimization strategies for the initial scheme are analyzed and proposed. The final scheme obtained by this distribution technique and these strategies have fewer switching times and lower offset frequency setting values. Additionally, this paper can lower the upper bound to 15 MHz to reduce the performance requirements of hardware devices such as phase readout circuits.

Section 2 of this paper elaborates on the operation process of a high-precision fitness genetic algorithm and presents offset frequency distribution schemes for the [6 MHz, 22 MHz] frequency domain. Within the frequency bounds and for a five-year mission, only 10 frequency switches are necessary. The shortest duration without a switch is 16 days, and the longest undisturbed measurement run would be 966 days. Section 3 shows that optimizing the frequency domain selection can narrow the reasonable frequency domain setting to [7 MHz, 17 MHz]. If the lower bound is not raised, the frequency domain can be controlled between [5 MHz and 15 MHz]. Furthermore, control of switch times ensures that the number of conversions for distribution schemes corresponding to frequency domains of [6 MHz, 17 MHz] and above is limited to between 6 and 13 times. The optimization of numerical settings results in an average overall reduction of 24.3% in the offset frequency values. Section 4 shows two final offset frequency distribution schemes for the different frequency domains in the simulated environment.

2. Generation of Frequency Distribution Schemes

In order to make the space gravitational wave detectors operate stably, our lab conducted orbit simulations to predict the Doppler shift for five years and included it as one of the inputs. Here, the genetic algorithm is combined with the beat frequency constraint and the corresponding phase-locking sequence [13]. Then individual adaptive evolution and elite domination are achieved through the corresponding fitness function. Eventually, we can obtain a frequency distribution scheme that conforms to the current conditions. We are aware of the fact that other algorithms exist that may be more efficient [16]. However, compared to other traditional heuristic algorithms, the global search space, robustness and fast convergence characteristics of genetic algorithm are exactly what we need.

Most genetic algorithms utilize a random method for generating initial populations. However, for space gravitational wave detection, it is essential to confine the initial population within a predetermined reasonable frequency domain to achieve rapid convergence to the optimal solution. Therefore, this paper constrains the generation of the initial popula-

tion, mainly involving steps such as random generation, constraint assessment, elimination, and fitness sorting. Based on the initial population, an iterative process is established through selection, crossover, and mutation to obtain the next generation with better quality than the previous until completion. The calculation flow is shown in Figure 1.

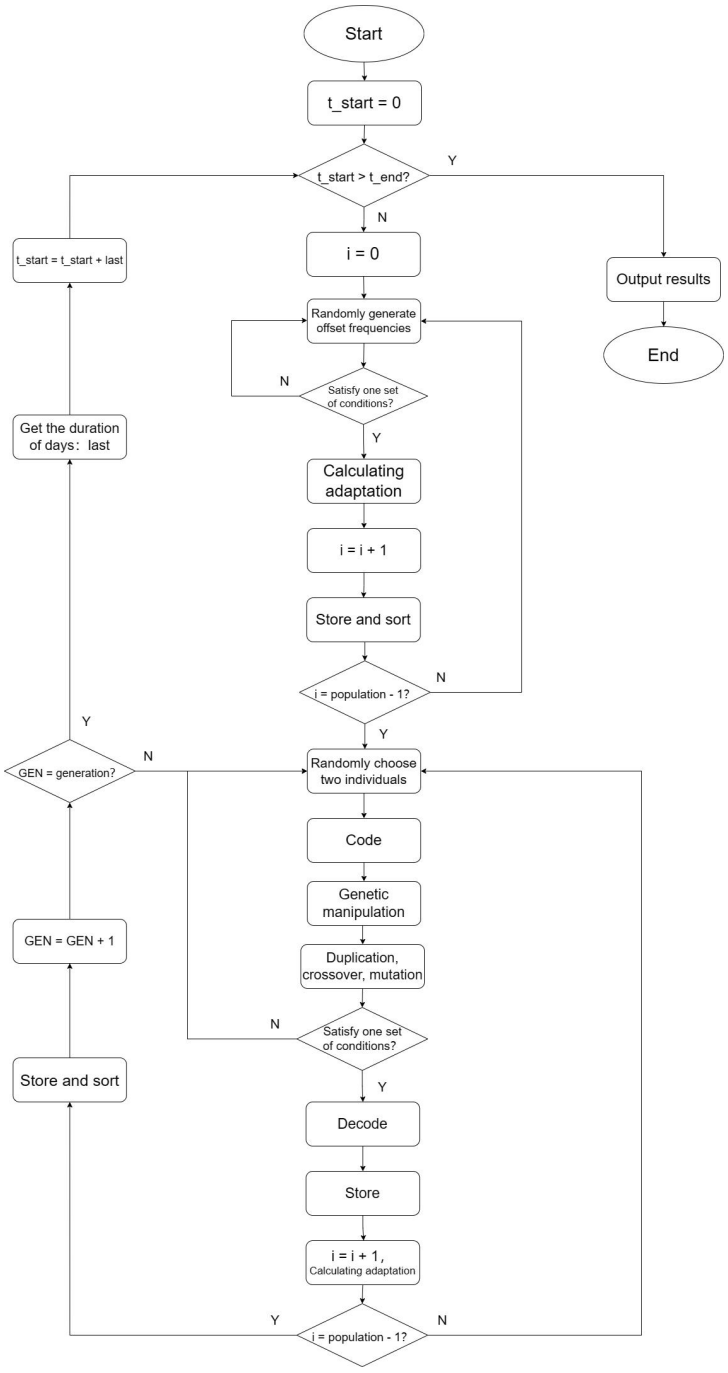

Figure 1. Genetic Algorithm Flow Chart for Distribution Scheme.

(1) Set the algorithm parameters, including population, generation, percentage of births allowed, mutation probability, mutation effective position and reorganization probability;

(2) Define the fitness function. To better distinguish high-quality individuals with similar results, we define the fitness function as the deviation between beat frequencies (f_n) and the midpoint of the set frequency domain(f_m) as in example 1:

$$F = C_{last} - C_{start} - \sum_{n=1}^{C_{last}-C_{start}} \frac{\sum_{n=1}^{N}(f_n - f_m)^3}{9 \times (f_m)^3}, \quad (1)$$

where C_{last} is the number of days that the group of offset frequency individuals can reach, C_{start} denotes the starting day for this group of offset frequencies.

(3) Randomly generated initial population. There are five offset frequencies in each individual. Then calculate the frequencies of beat notes and sort individuals by fitness;

(4) Code Mapping Decimal Offset Data to 16-bit Binary Numbers;

(5) Selection, crossover and mutation of primordial populations according to setting probability;

(6) Decode. The decimal real-valued solution corresponding to the binary number T is X, the conversion formula is shown in example 2 of equation:

$$X = a + T \times (b - a)/(2^n - 1), \quad (2)$$

where $[a, b]$ is the reasonable frequency domain and n is the binary length;

(7) Calculate and rank the fitness;

(8) If complete the scheduled number of iterations, go to step (9). Otherwise, go to step (4);

(9) If complete the number of days in the set year, end. Otherwise, go to step (3).

When locking the entire system according to the phase-locked scheme ① and frequency domain range [6 MHz, 22 MHz], we can obtain a specific distribution scheme as shown in Table 1. Each group of this scheme generates an optimal set of offset frequencies after 20 generations of inheritance so that it lasts as long as possible under setting conditions. In the next five years, only 10 frequency switches will be necessary. The shortest duration without a switch is 16 days, the longest undisturbed measurement run would be 966 days if no other events cause a short-time failure of the phase-locking. After several tests with the same parameters, although the offset frequency varies individually, the overall number of transitions and duration of days remains consistent, which guarantees the feasibility of the algorithm.

Table 1. Distribution Scheme.

Start	Δf1	Δf2	Δf3	Δf4	Δf5	Last
0	13.99	−12.99	−14.62	−14.61	12.99	227
227	−20.99	−10.99	−12.99	19.75	14.98	966
1193	−14.49	−15.99	14.99	15.99	−13.99	55
1248	−13.99	−15.99	15.99	18.99	−13.75	294
1542	16.99	9.99	15.81	−13.99	14.99	49
1591	17.99	14.02	11.99	−9.99	11.84	18
1609	6.99	−13.99	−13.99	−20.78	−15.49	16
1625	13.99	−8.99	−12.99	−13.99	−12.24	90
1715	14.98	−15.99	13.62	12.99	12.49	97
1812	13.99	14.99	10.81	14.99	13.99	>12

In this way, we can generate the corresponding distribution scheme under different frequency domains. Subsequently, we evaluate which distribution scheme is optimal based on factors such as the offset frequency duration, the number of switching, and the possibility of low-frequency optimization.

3. Optimization of Distribution Scheme

Through the above method, we can obtain the corresponding scheme for the set parameters. However, The scheme generated in such a state largely lacks a comprehensive consideration of the switch times and the low-frequency requirements of the phase readout circuit. This requires further optimizations on the bias frequency distribution scheme based

on the genetic algorithm. The optimization strategy will be described in the following three aspects: frequency domain selection extension, switch times control, and numerical low frequency.

3.1. Optimization of Frequency Domain Selection Extension

The three spacecraft in Taiji totally have six sets of interferometric links [17]. After determining the fixed frequency for the main laser, five offset frequencies are added to correct for the Doppler shift and to lock the other five lasers sequentially. The setting of its locking order is the phase-locking scheme. Different locking schemes have different effects on the beat note. The resulting distribution scheme will be also distinct.

The common phase-locking scheme in the current Taiji is shown as scheme ① in Figure 2 [13]. Laser A onboard spacecraft S1 is chosen to be the main laser and the frequency is constant at f0. Laser B on board the same spacecraft and laser F onboard spacecraft S3 is locked to A. Laser E is locked to laser F. Laser C onboard spacecraft S2 locks through laser B, and laser D on the same spacecraft S2 is locked to C. That completes the locking of the six lasers. The locked lines on both sides of the phase-locked scheme ① are completely symmetric and do not affect each other and are, therefore, the preferred scheme for each gravitational wave detection program.

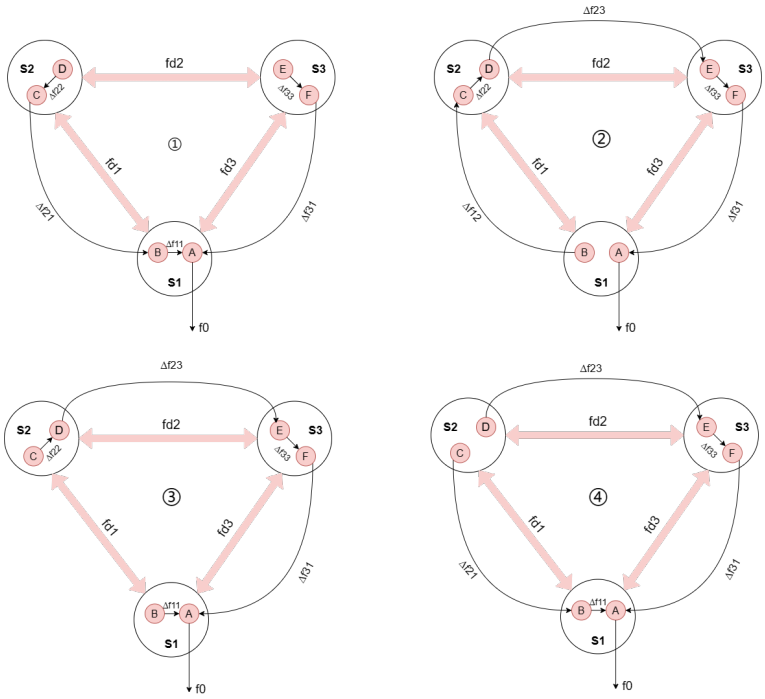

Figure 2. Phase-locking Schemes.

Scheme ① is suitable for most reasonable frequency domains. However, it may not be satisfied when the domain of the system is set more strictly. In the [7 MHz, 21 MHz] region, a suitable offset frequency will not be found after 1581 days to keep the beat frequencies within the setting domain. This is the time that the phase-locking scheme needs to be modified. Figure 2 also shows the other different locking sequences for gravitational wave detection. Three options all use laser A as the master laser, with adaptive offset frequencies added at various points to complete the locking [9].

We can calculate the beat frequency received by each interference system according to the order of the locking scheme. All locking processes in the figure have their own adaptive offset frequencies from Δf_{11} to Δf_{33}. The complete setting of these five parameter values over the five years of observatory operation is the offset frequency distribution scheme. f_{d1} to f_{d3} is the Doppler shift. The beat frequencies received by each interferometric platform

are $f_{AB,1}(t)$ to $f_{DE,2}(t)$. The equation relationship between these three types of parameters is also one of the constraints on the offset frequency setting and is called the phase locking equation. The following Equations (3)–(6) are listed for locking schemes ①, ②, ③ and ④, respectively.

$$f_{AB,1}(t) = \Delta f_{11} \tag{3a}$$
$$f_{AF,3}(t) = \Delta f_{31} \tag{3b}$$
$$f_{AF,1}(t) = \Delta f_{31} + 2 \times f_{d3}(t) \tag{3c}$$
$$f_{BC,2}(t) = \Delta f_{21} \tag{3d}$$
$$f_{BC,1}(t) = \Delta f_{21} + 2 \times f_{d1}(t) \tag{3e}$$
$$f_{EF,3}(t) = \Delta f_{33} \tag{3f}$$
$$f_{CD,2}(t) = \Delta f_{22} \tag{3g}$$
$$f_{DE,3}(t) = \Delta f_{31} + \Delta f_{33} + f_{d3}(t) - (\Delta f_{11} + \Delta f_{21} + \Delta f_{22} + f_{d1}(t) + f_{d2}(t)) \tag{3h}$$
$$f_{DE,2}(t) = f_{d3}(t) + f_{d2}(t) + \Delta f_{31} + \Delta f_{33} - (\Delta f_{11} + \Delta f_{21} + \Delta f_{22} + f_{d1}(t)) \tag{3i}$$

$$f_{AB,1}(t) = \Delta f_{31} + \Delta f_{33} + f_{d3}(t) + \Delta f_{11} + \Delta f_{21} + \Delta f_{22} + f_{d1}(t) + f_{d2}(t) \tag{4a}$$
$$f_{AF,3}(t) = \Delta f_{31} \tag{4b}$$
$$f_{AF,1}(t) = \Delta f_{31} + 2 \times f_{d3}(t) \tag{4c}$$
$$f_{BC,2}(t) = \Delta f_{12} + 2 \times f_{d1}(t) \tag{4d}$$
$$f_{BC,1}(t) = \Delta f_{12} \tag{4e}$$
$$f_{EF,3}(t) = \Delta f_{33} \tag{4f}$$
$$f_{CD,2}(t) = \Delta f_{22} \tag{4g}$$
$$f_{DE,3}(t) = \Delta f_{23} + f_{d2}(t) \tag{4h}$$
$$f_{DE,2}(t) = \Delta f_{23} \tag{4i}$$

$$f_{AB,1}(t) = \Delta f_{11} \tag{5a}$$
$$f_{AF,3}(t) = \Delta f_{31} \tag{5b}$$
$$f_{AF,1}(t) = \Delta f_{31} + 2 \times f_{d3}(t) \tag{5c}$$
$$f_{BC,2}(t) = \Delta f_{11} + f_{d1}(t) - (\Delta f_{31} + \Delta f_{22} + \Delta f_{23} + f_{d2}(t) + f_{d3}(t) + \Delta f_{33}) \tag{5d}$$
$$f_{BC,1}(t) = \Delta f_{11} - (\Delta f_{33} + f_{d3}(t) + \Delta f_{31} + \Delta f_{23} + \Delta f_{22} + f_{d1}(t) + f_{d2}(t)) \tag{5e}$$
$$f_{EF,3}(t) = \Delta f_{33} \tag{5f}$$
$$f_{CD,2}(t) = \Delta f_{22} \tag{5g}$$
$$f_{DE,3}(t) = \Delta f_{23} + 2 \times f_{d2}(t) \tag{5h}$$
$$f_{DE,2}(t) = \Delta f_{23} \tag{5i}$$

$$f_{AB,1}(t) = \Delta f_{11} \tag{6a}$$
$$f_{AF,3}(t) = \Delta f_{31} \tag{6b}$$
$$f_{AF,1}(t) = \Delta f_{31} + 2 \times f_{d3}(t) \tag{6c}$$
$$f_{BC,2}(t) = \Delta f_{21} \tag{6d}$$
$$f_{BC,1}(t) = \Delta f_{21} + 2 \times f_{d1}(t) \tag{6e}$$
$$f_{EF,3}(t) = \Delta f_{33} \tag{6f}$$
$$f_{CD,2}(t) = \Delta f_{31} + f_{d2}(t) + \Delta f_{23} + \Delta f_{33} + f_{d3}(t) - (\Delta f_{21} + f_{d1}(t) + \Delta f_{11}) \tag{6g}$$
$$f_{DE,3}(t) = \Delta f_{23} + 2 \times f_{d2}(t) \tag{6h}$$
$$f_{DE,2}(t) = \Delta f_{23} \tag{6i}$$

In addition to the above schemes, the different choices of master laser and different orbital positions of the spacecraft can also lead to the generation of different distribution schemes, named the orbital alignment pattern of the detection system. A complete orbital alignment pattern consists of the following six types from A1 to E2. A indicates that laser A on spacecraft S1 is the main laser with a constant frequency. The other lasers are thus locked to the frequency of laser A. C is dominated by laser C on spacecraft S2, and E is dominated by laser E on spacecraft S3. Figure 3 shows the complete orbital alignment pattern when laser A, C and E are the main lasers.

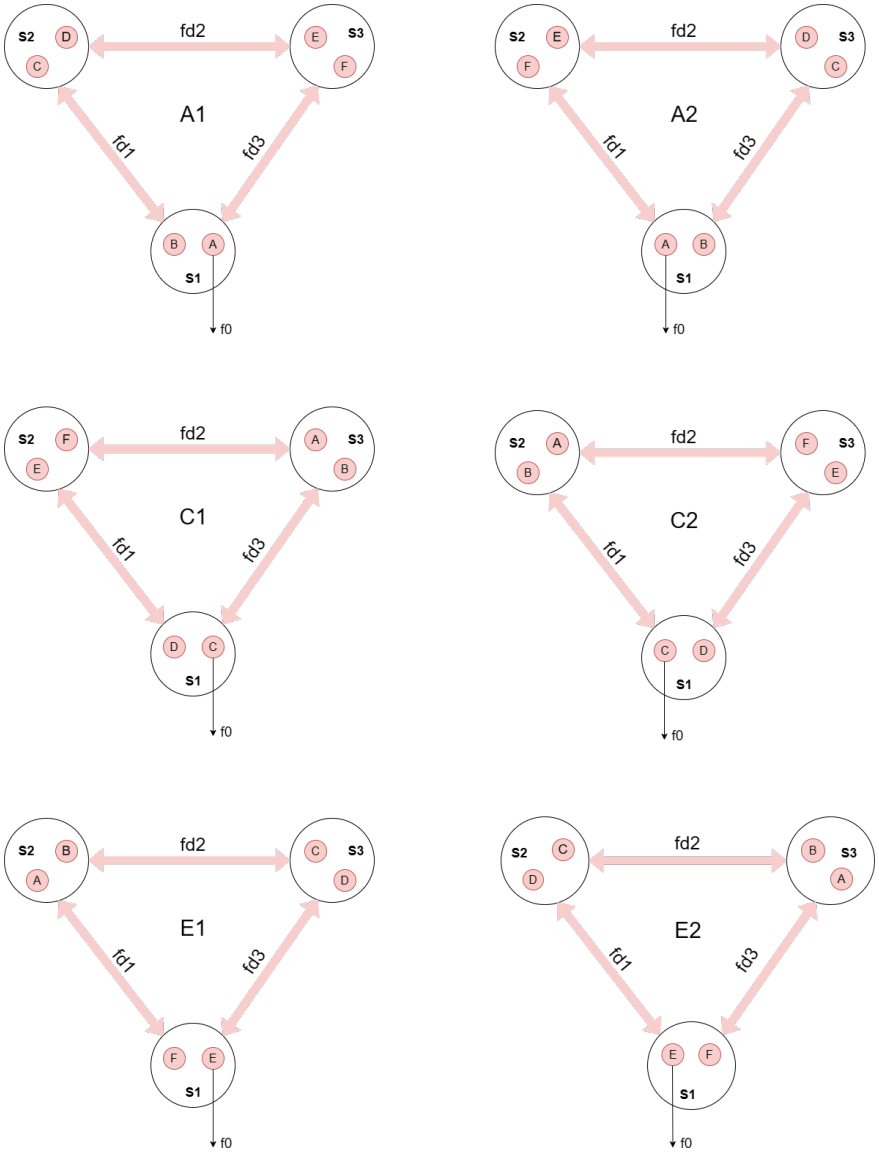

Figure 3. Complete Alignment Pattern.

The offset frequency distribution schemes generated by different phase-locking schemes in the [5 MHz, 25 MHz] frequency domain and alignment pattern A1 setting are shown in Figure 4. The distribution schemes given in each phase-locking scheme in the figure are all different from each other. Scheme ① requires only three frequency switches. The other three schemes switch at roughly the same time and number of times. They all require frequency switching five times, and the switching nodes are only two to three days apart. All four schemes can generate the complete frequency scheme under the current setting, and all of them can be considered for use. However, scheme ① has the highest priority.

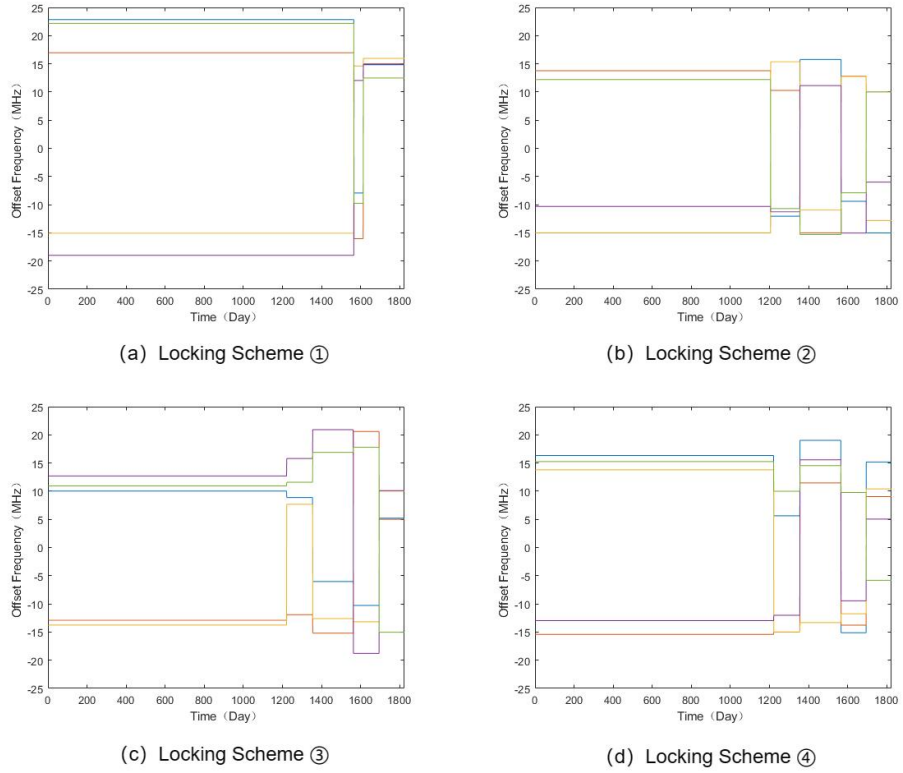

Figure 4. Distribution Frequency for Different Phase Locking Schemes.

Figure 5 shows the distribution scheme generated by the six alignment patterns in the [5 MHz, 25 MHz] frequency domain and the phase-locking scheme ① setting. The five lines indicate the five offset frequencies. The complete generation of the scheme demonstrates the feasibility of the six alignment patterns and the underlying genetic algorithm.

The offset frequency groups of alignment A1 and E2 are both converted three times. Other schemes generated by A2, C1, C2 and E1 are extremely similar, with the difference in the number of conversion days for the frequency groups being around one or two days.

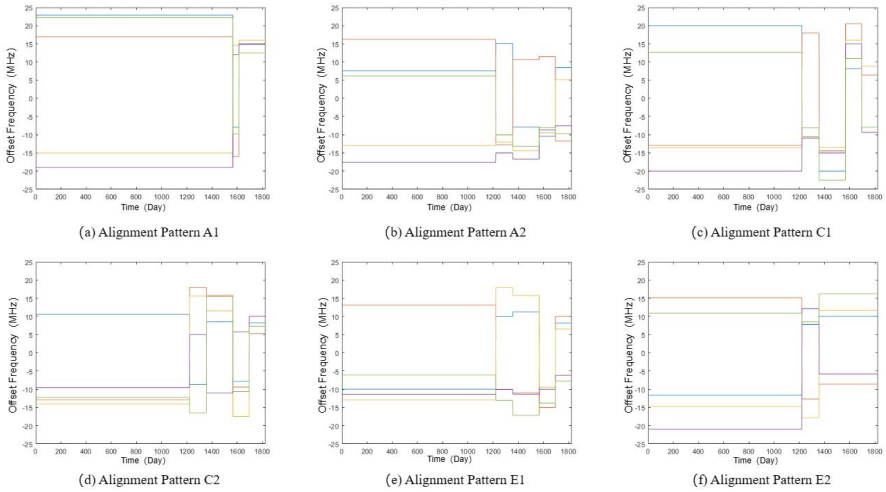

Figure 5. Distribution Frequency of Different Alignment Patterns.

This optimization method not only offers more options for phase-locked schemes and alignment patterns under various frequency domain settings but also enriches the selection of frequency domains. Experiments show that when the frequency domain is set too narrow, there is no fixed offset frequency to keep the beat frequencies within its range.

The smallest acceptable frequency domain setting for phase-locking scheme ① is [7 MHz, 22 MHz]. Moreover, the distribution scheme of the narrowest frequency domain is given by the phase-locking scheme ③. When the alignment pattern is C1, scheme ③ can satisfy the frequency scheme generation of [7 MHz, 17 MHz]. This setting requires 15 switching of the offset frequency group over five years, with a maximum duration of 503 days and a minimum duration of 40 days. If the lower bound is still set to 5 MHz without raising, the upper bound can be reduced to 15 MHz, at which point the program needs to be switched 16 times with a minimum and maximum offset frequency duration of 40 days and 266 days. It is already the frequency limit achievable by the current distribution scheme.

3.2. Optimization of Switch Times Control

In Taiji, the three-star formation will be in orbit for five years. During this period the offset frequency needs to be switched regularly to ensure the proper operation of the detector. However, the process of regularly switching results in a loss of the laser lock and renders the observatory non-operational for a short while. In the research process of this paper, it was found that there are certain problems to be solved when there are too many or too few conversions.

When the setting frequency domain is set too small, the resulting distribution scheme will involve excessive switching, and there could even be cases where the set values for a frequency group only last for one or two days. The scheme when the frequency domain is set to [7 MHz, 22 MHz] is shown in Figure 6. The program needed to switch offset frequencies 16 times in five years and switched six times between 1586 and 1622, with the longest duration being just 8 days and the shortest lasting 2 days. This number of switches seriously affects the detection of gravitational waves in this time period, so the choice of the phase-locking scheme and alignment pattern cannot be limited to the current one.

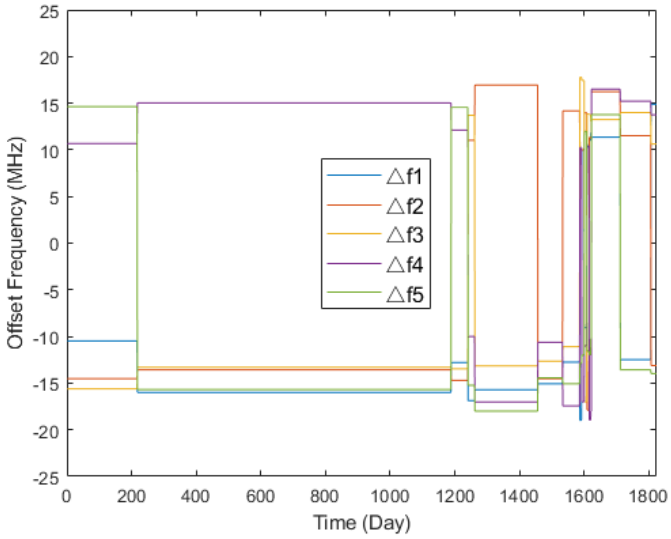

Figure 6. Raw Offset Frequency Setting of [7 MHz, 22 MHz].

When the set frequency domain is too wide, as Figure 7 shows the distribution scheme at [5 MHz, 25 MHz]. The data in the first stage have remained unchanged for 1565 days. This also results in the individual frequencies of the scheme being too close to the upper bound of 25 MHz in the frequency domain, which is not conducive to the performance requirements of other hardware systems. If the current distribution scheme does not meet the combined requirements of the current software and hardware. It can be optimized by changing the phase-locking scheme and the arrangement pattern. Twenty-four schemes are obtained by permutation, among which the optimal one is chosen.

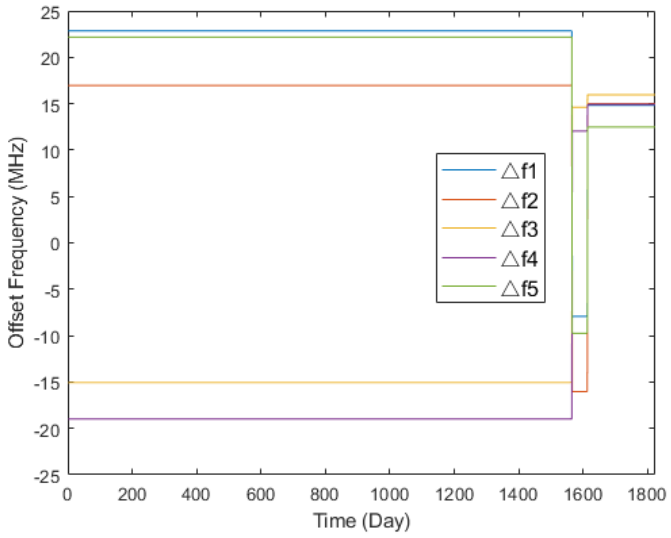

Figure 7. Raw Offset Frequency Setting of [5 MHz, 25 MHz].

Figure 8 shows the results of the generation test of the offset frequency distribution scheme for each frequency band, where the left-hand side indicates the minimum value of the set frequency domain and the upper part indicates its maximum. The test parameters were set to arm length of 3 million kilometers, Doppler shift in 5 years and most commonly used locking scheme ①. Green stands for the frequency range in which the distribution scheme can be generated properly where the number of switches between 6 and 13. The duration of each set of offset frequencies is 7 days or more. Yellow implies insufficient switches. This leads to relatively high values for the offset frequency settings corresponding to the first stage, which can be further optimized. Red means two conditions that no set of offset frequencies could be found to keep all beat frequencies within the given frequency bounds or excessive switches exist. Excessive switches will always leave the interferometric links in a long unlocked state and affect the detection accuracy. In this case, the phase-locking scheme or alignment pattern needs to be changed.

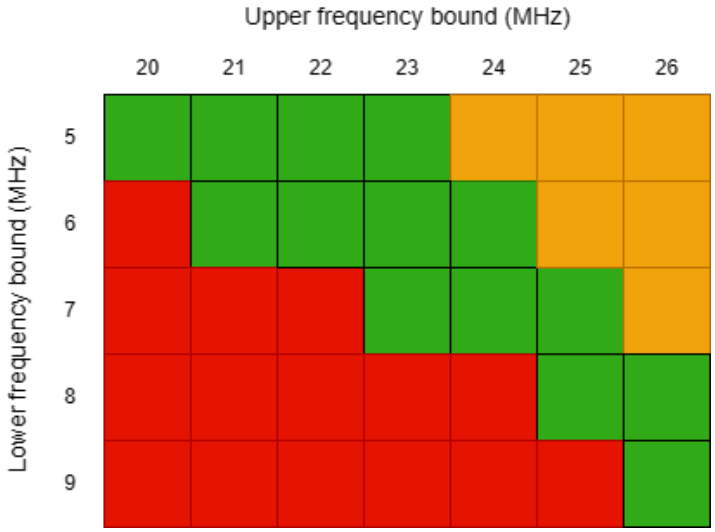

Figure 8. Possible Number of Conversions in Different Frequency Domains.

Therefore, the number of conversions is judged and optimized after the scheme has been generated. The following content displays the optimization process of the frequency

domain [7 MHz, 22 MHz] with excessive conversions and [5 MHz, 25 MHz] with insufficient conversions. The optimization effect is shown in Figures 9 and 10.

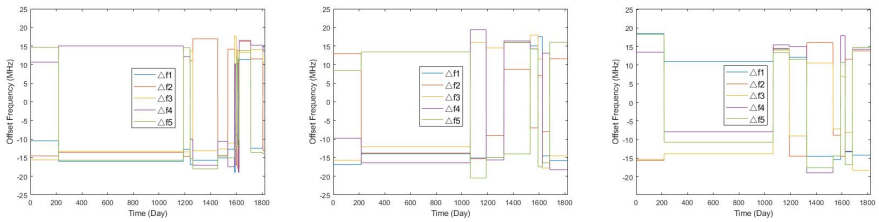

(a) 7 MHz – 22 MHz before optimization (b) 7 MHz – 22 MHz scheme optimization (c) 7 MHz – 22 MHz alignment optimization

Figure 9. Solution Optimization Comparison of [7 MHz, 22 MHz].

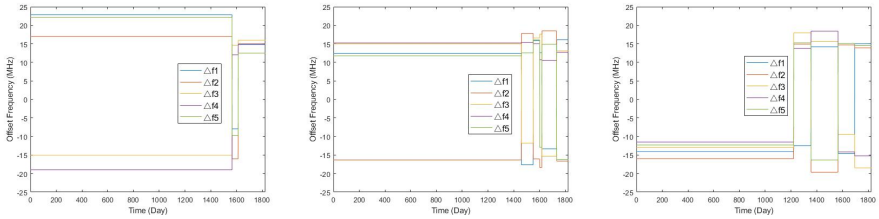

(a) 5 MHz – 25 MHz before optimization (b) 5 MHz – 25 MHz scheme optimization (c) 5 MHz – 25 MHz alignment optimization

Figure 10. Solution Optimization Comparison of [5 MHz, 25 MHz].

Figure 9a–c show the comparison in the frequency domain [7 MHz, 22 MHz]. The frequency in Figure 9a needs to be converted 16 times. During the period from 1586 to 1622, the longest duration is only 8 days and the shortest is 2 days. Figure 9b uses the scheme ③ without changing the alignment pattern, which requires only nine conversions, with the longest lasting 848 days and the shortest lasting 33 days so that its switch times and durations are more reasonable. On the contrary, Figure 9c uses the alignment E1 of Figure 3 without changing the locking scheme. The number of conversions and switching time nodes of Figure 9c are similar to those of Figure 9b. Since scheme ① is the preferred scheme for the whole system. By comparing the two options, Figure 9b with phase-locked scheme ① with the alignment E1 is the better choice when the frequency domain is restricted to the range of [7 MHz, 22 MHz].

Figure 10a–c show the comparison in the frequency domain at 5 MHz–25 MHz. In Figure 10a, only three frequency switches are made in five years, and the offset frequency is too close to the upper bound of the frequency domain. Figure 10b performs a reduction operation on the frequency domain to achieve a lower offset frequency by appropriately reducing the duration of each segment. Figure 10c changes the choices of alignment pattern to alignment C2. The number of analyses for the above tests should be kept between 6 and 13 as much as possible. In this case, the best solution is obtained by using scheme ① and reducing the reasonable frequency domain appropriately.

In order to fully explore the possible frequency domain range settings, we traversed three additional phase-locking schemes and six alignment patterns based on the above reasonable intervals for the number of conversions. The results are shown in Figure 11.

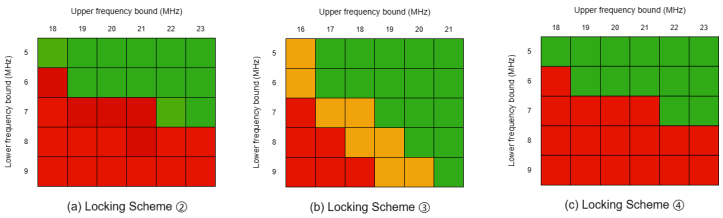

(a) Locking Scheme ② (b) Locking Scheme ③ (c) Locking Scheme ④

Figure 11. Number of Conversions in Each Frequency Domain of The Scheme ③.

The green parts show the frequency bands for which a complete frequency distribution scheme can be generated. The number of transitions is all kept within a reasonable range of 6–13. Yellow can generate complete frequency distribution schemes, but the switch is more than 13. The red color indicates the inability to generate a complete scheme. The phase-locking scheme ② in Figure 11a is consistent with scheme ④ in Figure 11c, with an acceptable minimum frequency domain of [6 MHz, 19 MHz]. Scheme ③ accepts a narrower frequency domain range, specifically [6 MHz, 17 MHz]. It is also the minimum frequency domain for a reasonable number of conversions.

3.3. Optimization of Low Frequency

The phase readout circuit is used to demodulate the beat notes received by each laser heterodyne interferometry platform. Due to the accuracy requirements for Program Taiji, the lower the frequency band, the lower the phase noise. Therefore, in order to improve the phase readout accuracy and increase its signal resolution sensitivity, the low-frequency band is optimized on the basis of the originally generated frequency distribution scheme.

In the scheme generation described above, the individual adaptation is determined by the degree of convergence dispersion of the frequencies of the nine beat frequencies with respect to the median value. This leads to higher values for some offset frequency settings. For distribution schemes with wider frequency domains and the number of switches below the reasonable range, it is more necessary to optimize. According to the statistical analysis index, its concentration trend is used to bring the reproductive offspring in the genetic algorithm closer to the low-frequency band. This method does not have a significant impact on the number of conversions and the duration of the distribution plan. That is to say, it is applicable in the full frequency range.

In this paper, the genetic algorithm produces the last generation of high-quality individuals with extremely close values of the offset frequency. So, we distinguish individual differences more carefully by appropriately increasing the accuracy of the fitness function. Under the reasonable frequency domain setting $[f_{min}, f_{max}]$, we further modify the deviation calculation in the fitness function, and the result is shown in example (7).

$$F_N = F_{N-1} + \frac{\sum_{n=1}^{N}(f_n - \overline{f})^3}{9 \times (\overline{f})^3}, \tag{7}$$

$\overline{f}$ is the convergence value, which represents the current frequency value that we would like the nine-beat notes to be close. It can be set through the parameter interface and is calculated as shown in example (8).

$$\overline{f} = \frac{f_{max} - f_{min}}{x} + f_{min} \tag{8}$$

Since four of the nine beat notes change with each day's Doppler shift, the degree of deviation is calculated for each day and summed. F_N represents the sum of all deviations from the convergence value up to the current day number. F_{N-1} represents the sum until the previous day. N is the overall number of days that the set of offset frequency groups can be maintained. The fractional equation calculates the mean square deviation of the nine beat notes with respect to the convergence value to measure the degree of deviation of the beat notes. Finally, F_N and N need to be divided to calculate the average fitness which is used to compare individuals with the same number of days N. The smaller the value of the average degree of deviation of an individual under this method of calculation, the higher the population fitness of the individual and the higher the survival rate.

Accordingly, a further optimization comparison of the solutions is shown in Figure 12 in the same reasonable frequency domain, phase-locking scheme and arrangement. The graph is represented by the average of the frequency groups' absolute values. We can obtain such significant optimization results.

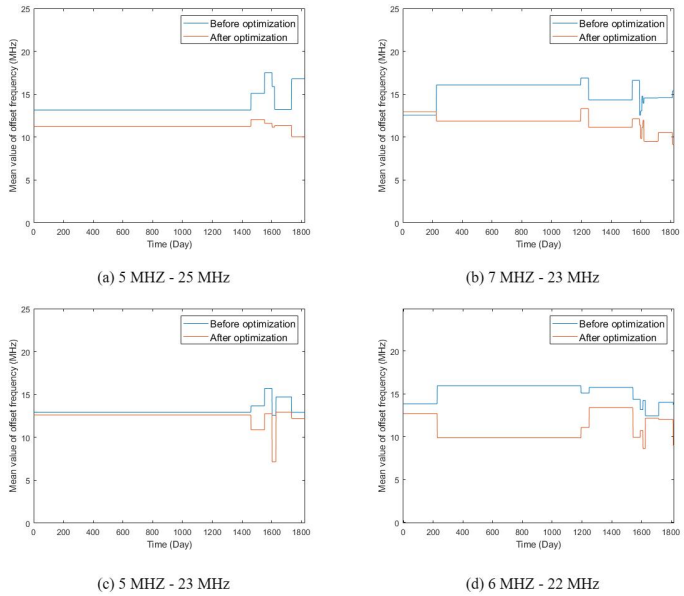

Figure 12. Comparison of Different Frequency Band Distribution Schemes After Low Frequency Optimization.

4. Results and Discussion

Based on the above approach, this paper shows the optimal offset frequency distribution for the two reasonable frequency domains [5 MHz, 25 MHz] and [7 MHz, 21 MHz].

Table 2 shows the optimal distribution scheme for [5 MHz, 25 MHz], using locking scheme ①, and the alignment is A1. Figure 13 shows its offset frequency transformation curve and the remaining four time-varying beat frequencies curves. It is optimized by narrowing the reasonable frequency domain. The scheme is switched six times in total and the longest one lasting 1459 days. Although the final result increases the number of switches, the increase will not significantly impact the continuous observations within the five years. In addition, we have greatly reduced the overall setting of the offset frequency value, which improves the result of Zhang [13] with the same settings, for which some offset frequency values are close to the upper bound of 25 MHz. For the offset frequency setting over a five-year period, a reduction of 20.93% is achieved.

Table 2. Offset Frequency Distribution Scheme of 5 MHz–25 MHz.

Start	Δf1	Δf2	Δf3	Δf4	Δf5	Last
0	10.57	−15.29	−15.09	−6.50	−10.72	1459
1459	12.34	17.02	15.89	−16.14	12.63	92
1551	−14.44	−13.60	−8.89	−8.31	−9.72	50
1601	−7.93	11.63	6.07	9.96	7.35	17
1618	10.90	−14.25	12.11	−8.94	−10.48	115
1733	11.34	11.22	9.99	−11.03	−13.66	91

Table 3 shows the optimal distribution scheme for [7 MHz, 21 MHz], using locking scheme ③, and the alignment is E1. Figure 14 shows two frequency curves. Since all the alignment patterns of scheme ① cannot find a suitable offset frequency to form a complete distribution scheme. The final solution uses the scheme ③. After low-frequency optimization, the distribution scheme is switched seven times in total and the longest one lasting 1015 days, which substantially improves the results of Barke [9], for which the offset frequency can remain unchanged for up to 177 days and the number of frequency switches can reach 24.

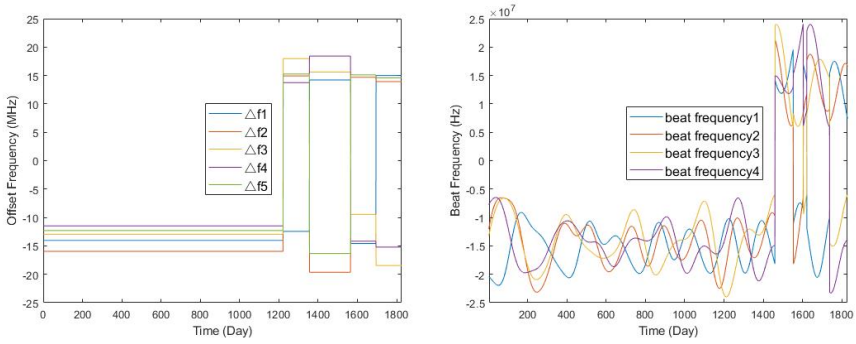

(a) Offset Frequency (b) Time-varying Beat Frequency

Figure 13. Beat Frequency Curve of [5 MHz, 25 MHz].

Table 3. Offset Frequency Distribution Scheme of 7 MHz–21 MHz.

Start	Δf1	Δf2	Δf3	Δf4	Δf5	Last
0	8.48	14.00	12.23	−11.81	−14.93	208
208	12.49	12.50	−12.31	14.79	10.33	1015
1223	12.11	−14.07	9.56	7.53	−7.88	118
1341	7.56	−12.26	15.04	8.80	10.50	182
1523	−12.44	−13.84	−9.44	−14.53	10.62	56
1579	16.06	14.06	10.76	−16.09	−11.40	98
1677	14.41	13.13	10.54	−8.65	−8.85	147

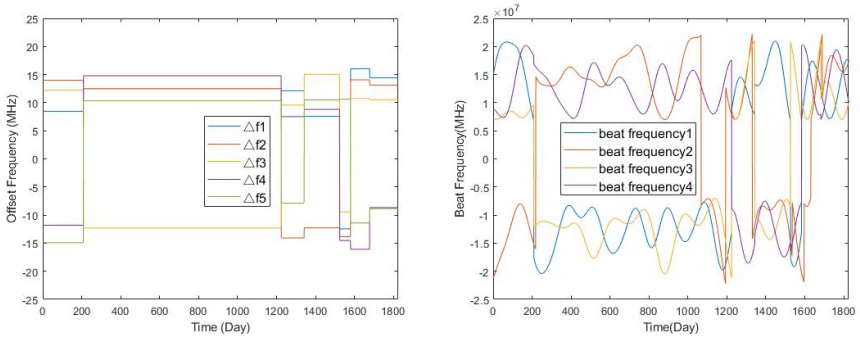

(a) Offset Frequency (b) Time-varying Beat Frequency

Figure 14. Beat Frequency Curve of [7 MHz, 21 MHz].

5. Conclusions

The present study investigates an offset frequency distribution scheme to mitigate the impact of Doppler shift between spacecraft in the orbital position of the three-star system. Firstly, by analyzing the potential reasonable frequency domains, the overall process of the improved genetic algorithm is elucidated. The generation of the offset frequency distribution scheme under the [6 MHz, 22 MHz] range is enumerated. After conducting 200 individuals per generation and reproducing for 20 generations, the final scheme needs to be switched 10 times and can last for a maximum duration of 966 days and a minimum duration of 16 days. This ensures effective long-term detection of gravitational waves.

Secondly, three optimization strategies based on the initial scheme are proposed: frequency domain selection extension strategy, switch times control strategy and low-frequency optimization strategy. The first optimization strategy verifies the feasibility of each phase-locking scheme and alignment pattern. It also identifies the frequency setting minimum thresholds as [5 MHz, 15 MHz] and [7 MHz, 17 MHz]. The number of conversions for distribution schemes corresponding to the frequency domains [6 MHz, 17 MHz] and above can be controlled to be between 6 and 13 conversions after switch times optimization. Low-frequency optimization results in a general reduction of 25.4% of

offset frequencies. Finally, the above methods are used to enumerate the offset frequency distribution schemes for heterodyne interference of the [5 MHz, 25 MHz] and [7 MHz, 21 MHz] frequency domains. These schemes will provide reliable references for further optimization of frequency distribution issues for Program Taiji.

However, the schemes provided in this paper are mainly based on simulation, and specific experimental verification is not included. Due to the complexity of the interstellar gravitational wave detection observatory, it is still difficult for the ground to simulate the exact same environment as the Universe during the five-year operational cycle for the validation of the simulation data. The technical challenges of the ground simulation are mainly related to phase-locking and inter-satellite optical links. On the one hand, the ground is unable to simulate the loss of laser lock and identify the positive and negative of the beat frequency. On the other hand, the loss of phase lock in inter-satellite optical links can result in the failure of differential wavefront sensing (DWS) technology, thereby leading to the failure of acquisition tracking and pointing (ATP). These challenges require strategies such as high-precision sensors, adaptive algorithms and advanced digital signal processing techniques and need to be discussed in detail in the following work.

Author Contributions: Conceptualization, H.L. and X.L.; Data curation, W.Y.; Methodology, L.Z. and W.Y.; Project administration, J.W. and X.L.; Software, L.Z.; Supervision, X.L.; Writing—original draft, L.Z.; Writing—review & editing, X.L. All authors have read and agreed to the published version of the manuscript.

Funding: This work is supported by the fund: National Key Research and Development Program of China (Grant No. 2023YFC2205401).

Institutional Review Board Statement: Not applicable.

Informed Consent Statement: Not applicable.

Data Availability Statement: The raw data supporting the conclusions of this article will be made available by the authors on request.

Conflicts of Interest: The authors declare no conflict of interest.

References

1. Ruan, W.H.; Guo, Z.K.; Cai, R.G.; Zhang, Y.Z. Taiji program: Gravitational-wave sources. *Int. J. Mod. Phys.* **2020**, *17*, 2050075. [CrossRef]
2. Bailes, M.; Berger, B.K.; Brady, P.R.; Branchesi, M.; Danzmann, K.; Evans, M.; Holley-Bockelmann, K.; Iyer, B.R.; Kajita, T.; Katsanevas, S.; et al. Gravitational-wave physics and astronomy in the 2020s and 2030s. *Nat. Rev. Phys.* **2021**, *5*, 344–366. [CrossRef]
3. Hu, W.R.; Wu, Y.L. The Taiji Program in Space for gravitational wave physics and the nature of gravity. *Natl. Sci. Rev.* **2017**, *4*, 685–686. [CrossRef]
4. Armstrong, J.W.; Estabrook, F.B.; Tinto, M. Time-delay interferometry for space-based gravitational wave searches. *Astrophys. J.* **1999**, *527*, 814. [CrossRef]
5. Li, H.J.; Qi, H.X.; Liang, X.D.; Zeng, L.X.; Yao, W.L.; Yang, Y.C.; Wang, J.Y. Automatic digital optical heterodyne phase locking loop in the milliradian domain for spaceborne laser interferometry. *Appl. Opt.* **2022**, *61*, 6915–6923. [CrossRef]
6. Heinzel, G.; Esteban, J.J.; Barke, S.; Otto, M.; Wang, Y.; Garcia, A.F.; Danzmann, K. Auxiliary functions of the LISA laser link: Ranging, clock noise transfer and data communication. *Class. Quantum Gravity* **2011**, *28*, 094008. [CrossRef]
7. Folkner, W.M.; Hechler, F.; Sweetser, T.H.; Vincent, M.A.; Bender, P.L. LISA orbit selection and stability. *Class. Quantum Gravity* **1997**, *14*, 1405. [CrossRef]
8. Oliver, G. Phase Readout for Satellite Interferometry. Ph.D. Thesis, Universitätsbibliothek Hannover, Hannover, Germany, 2014.
9. Simon, B. Inter-Spacecraft Frequency Distribution for Future Gravitational Wave Observatories. Ph.D. Thesis, Gottfried Wilhelm Leibniz Universität Hannover, Hannover, Germany, 2015.
10. Wissel, L.; Wittchen, A.; Schwarze, T.S.; Hewitson, M.; Heinzel, G.; Halloin, H. Relative-intensity-noise coupling in heterodyne interferometers. *Phys. Rev. Appl.* **2022**, *17*, 024025. [CrossRef]
11. McNamara, P.W. Weak-light phase locking for LISA. *Class. Quantum Gravity Int. J. Gravity Geom. Field Theor. Supergravity Cosmol.* **2005**, *22*, S243–S247. [CrossRef]
12. Diekmann, C.; Steier, F.; Sheard, B.; Heinzel, G.; Danzmann, K. Analog phase lock between two lasers at LISA power levels. *J. Phys. Conf. Ser.* **2009**, *154*, 012020. [CrossRef]

13. Zhang, J.; Yang, Z.; Ma, X.; Peng, X.; Liu, H.; Tang, W.; Zhao, M.; Gao, C.; Qiang, L.E.; Han, X.; et al. Inter-spacecraft offset frequency setting strategy in the Taiji program. *Appl. Opt.* **2022**, *61*, 837–843. [CrossRef] [PubMed]
14. Zhang, J.; Ma, X.; Zhao, M.; Peng, X.; Gao, C.; Yang, Z. Advanced inter-spacecraft offset frequency setting strategy for the Taiji program based on a two-stage optimization algorithm. *Appl. Opt.* **2023**, *62*, 4370–4380. [CrossRef]
15. Luo, Z.; Bai, S.; Bian, X.; Chen, G.; Dong, P.; Dong, Y.; Gao, W.; Gong, X.; He, J.; Li, H.; et al. Gravitational wave detection by space laser interferometry. *Adv. Mech.* **2013**, *43*, 415–447.
16. Beyer, H.G.; Sendhoff, B. Robust optimization–a comprehensive survey. *Comput. Methods Appl. Mech. Eng.* **2007**, *196*, 3190–3218. [CrossRef]
17. Luo, Z.; Guo, Z.; Jin, G.; Wu, Y.; Hu, W. A brief analysis to Taiji: Science and technology. *Results Phys.* **2019**, *16*, 2211–3797. [CrossRef]